APPLIED AND ENVIRONMENTAL MICROBIOLOGY, Nov. 2005, p. 7008–7018 Vol. 71, No. 11
0099-2240/05/$08.00+0 doi:10.1128/AEM.71.11.7008–7018.2005

Bacterial Community Dynamics and Polycyclic Aromatic Hydrocarbon Degradation during Bioremediation of Heavily Creosote-Contaminated Soil

Marc Viñas,[1] Jordi Sabaté,[1] María José Espuny,[2] and Anna M. Solanas[1]*

Department of Microbiology, University of Barcelona, Diagonal 645, E-08028 Barcelona, Spain,[1] and Department of Microbiology and Parasitology, University of Barcelona, Joan XXIII, s/n, E-08028 Barcelona, Spain[2]

Received 27 December 2004/Accepted 19 July 2005

Bacterial community dynamics and biodegradation processes were examined in a highly creosote-contaminated soil undergoing a range of laboratory-based bioremediation treatments. The dynamics of the eubacterial community, the number of heterotrophs and polycyclic aromatic hydrocarbon (PAH) degraders, and the total petroleum hydrocarbon (TPH) and PAH concentrations were monitored during the bioremediation process. TPH and PAHs were significantly degraded in all treatments (72 to 79% and 83 to 87%, respectively), and the biodegradation values were higher when nutrients were not added, especially for benzo(*a*)anthracene and chrysene. The moisture content and aeration were determined to be the key factors associated with PAH bioremediation. Neither biosurfactant addition, bioaugmentation, nor ferric octate addition led to differences in PAH or TPH biodegradation compared to biodegradation with nutrient treatment. All treatments resulted in a high first-order degradation rate during the first 45 days, which was markedly reduced after 90 days. A sharp increase in the size of the heterotrophic and PAH-degrading microbial populations was observed, which coincided with the highest rates of TPH and PAH biodegradation. At the end of the incubation period, PAH degraders were more prevalent in samples to which nutrients had not been added. Denaturing gradient gel electrophoresis analysis and principal-component analysis confirmed that there was a remarkable shift in the composition of the bacterial community due to both the biodegradation process and the addition of nutrients. At early stages of biodegradation, the α-*Proteobacteria* group (genera *Sphingomonas* and *Azospirillum*) was the dominant group in all treatments. At later stages, the γ-*Proteobacteria* group (genus *Xanthomonas*), the α-*Proteobacteria* group (genus *Sphingomonas*), and the *Cytophaga-Flexibacter-Bacteroides* group (*Bacteroidetes*) were the dominant groups in the nonnutrient treatment, while the γ-*Proteobacteria* group (genus *Xathomonas*), the β-*Proteobacteria* group (genera *Alcaligenes* and *Achromobacter*), and the α-*Proteobacteria* group (genus *Sphingomonas*) were the dominant groups in the nutrient treatment. This study shows that specific bacterial phylotypes are associated both with different phases of PAH degradation and with nutrient addition in a preadapted PAH-contaminated soil. Our findings also suggest that there are complex interactions between bacterial species and medium conditions that influence the biodegradation capacity of the microbial communities involved in bioremediation processes.

Polycyclic aromatic hydrocarbons (PAHs) are a class of fused-ring aromatic compounds that are ubiquitous environmental pollutants (13). Microorganisms play an important role in the degradation of PAHs in terrestrial and aquatic ecosystems, and microbial degradation is the main process in natural decontamination. Enhancement of this phenomenon is the basis of bioremediation technologies (2).

Microbial degradation of PAHs in soil is restricted by various factors that often result in a lower-than-expected bioremediation efficiency. One of these factors is the low bioavailability of the compounds. In a recent study (1) we described significant enhancement of the biodegradation of high-molecular-weight PAHs and alkylated derivatives of these compounds from Casablanca crude oil caused by a microbial consortium in the presence of a biosurfactant produced by *Pseudomonas aeruginosa* strain AT10. Another important factor in bioremediation of contaminated soils is the availability of nitrogen and phosphorus, which allows the necessary increase in the size of the hydrocarbon-degrading microbial populations.

Taking into account the fact that each contaminated site can respond in a different way to distinct parameters that affect microbial biodegradation, laboratory-scale bioremediation protocols have been developed in order to determine the effects of different conditions (30). In such feasibility studies, addition of nutrients, biosurfactants, exogenous inocula, or other additives can be assayed. Nevertheless, in almost all of these studies monitoring of the process is based on chemical analysis of contaminants. A better understanding of the diversity of the microbial communities inhabiting PAH-contaminated soils and their response to different biostimulation or bioaugmentation strategies could provide clues about the type of bacteria that are able to adapt to and exploit such habitats.

It is well known that the majority of microbes in environmental samples cannot be cultured at present in laboratory media, which are biased for the growth of specific microorganisms (5, 34). In light of this, molecular biological techniques offer new opportunities. For example, denaturing gradient gel electrophoresis (DGGE) allows us to directly determine the presence and relative levels of different 16S rRNA gene am-

* Corresponding author. Mailing address: Department of Microbiology, University of Barcelona, Diagonal 645, E-08028 Barcelona, Spain. Phone: (34) 93 4034623. Fax: (34) 93 4034629. E-mail: asolanas@ub.edu.

TABLE 1. Soil treatments

Code	Treatment[a]	Description
1M	Untreated "dry" soil	Soil with 1.63% water content corresponding to 5.8% WHC
2M	Basic	Aerated soil at 40% WHC
3M	Autoclaved soil	Autoclaved three times at 121°C for 21 min
4M	Nutrient[b]	Aerated soil at 40% WHC; KNO_3 and K_2HPO_4 added to give a final concentration equivalent to a C/N/P molar ratio of 300:10:1 from the total organic carbon
5M	Nutrient + biosurfactant[b]	Aerated soil at 40% WHC; nutrients; biosurfactant MAT10 added twice (days 0 and 130) at a final water interstitial concentration of 150 mg liter^{-1}[d]
6M	Nutrient + inoculum[b,c]	Aerated soil at 40% WHC; nutrients; polycyclic aromatic hydrocarbon-degrading consortium AM added five times (days 14, 26, 57, 120, and 165) so that there were 10^8 microorganisms g of soil^{-1} at each addition[e]
7M	Nutrient + iron octoate[b]	Aerated soil at 40% WHC; nutrients; ferric ion added as ferric octoate twice (days 0 and 145) as an oleophilic source of iron at a final interstitial water concentration of 250 μM[f]

[a] All treatments were carried out in triplicate in 1-liter sterile glass jars containing 600 g of sieved soil (<6 mm) and were aerated and moisture corrected by mixing twice a week.
[b] Nutrient amendment was carried out as follows: one-third of the total nutrient addition was performed at time zero, and the remaining two-thirds was added on days 45 and 90.
[c] Cells from consortium AM on day 6 of incubation were grown overnight in Erlenmeyer flasks containing 500 ml of tryptone soy broth to obtain an optical density at 600 nm of 0.8 (5×10^{10} total cells). Then the cells were harvested and washed in 0.85 M NaCl. The pellet was resuspended in 0.85 M NaCl and added to correct the water content in treatment 6M (approximately 30 ml).
[d] See reference 1 for a description of biosurfactant MAT10.
[e] See references 1 and 36 for a description of consortium AM.
[f] See reference 33.

plicons both qualitatively and semiquantitatively in order to perform a community analysis (15).

Although there has been much research on the bacterial community structure associated with bioremediation of different kinds of environmental pollutants (18, 23, 26), little is known about bioremediation of PAH-contaminated soils. The few studies that have been described to date have been performed either with soils with low levels of PAH contamination (6, 41, 28) or with spiked soils (32), and there has not been accurate monitoring of the microbial population dynamics throughout the biodegradation process.

To assess both the potential of bioremediation in a heavily PAH-contaminated soil and the effects of different treatments on the bacterial community structure, we used a series of bioremediation treatments in microcosm experiments. An old, loamy clay soil that was heavily contaminated with PAH-creosote (~8,000 mg total petroleum hydrocarbon [TPH] kg of soil^{-1}, including 2,700 mg resolved PAH kg of soil^{-1}) was subjected to different treatments. Degradation of the PAHs and TPH of creosote was monitored. The bacterial community was studied by culture-independent analysis of 16S rRNA genes by means of DGGE (25) and determination of the most probable number (MPN) of heterotrophs and PAH degraders in the microbial population (39).

MATERIALS AND METHODS

Soil analysis. A composite sample of creosote-contaminated soil (50 kg) from a wood treatment plant near Barcelona, Spain, was obtained from the top 20 cm and sieved (<6 mm). The soil texture was determined by sedimentation analysis (16). The primary dissolved inorganic constituents of a saturated paste extract (nitrate, nitrite, ammonia, phosphorus) were determined using ion chromatography (30). The soil moisture content, water-holding capacity (WHC), electrical conductivity, total organic carbon content, total nitrogen content, and pH were determined as described previously (30).

Seven different treatments in microcosms experiments designated 1M to 7M were used in the study, as shown in Table 1. To determine the best soil water content for use in the microcosm experiments, five different water contents (5%, 20%, 40%, 60%, and 75% WHC) and autoclaved soil as an abiotic control were assayed for 15 days in triplicate in miniaturized microcosms with the nutrient additions described in Table 1. The best results ($P < 0.05$) were observed with 40% and 60% WHC (22 to 27% biodegradation of TPH), while with 20% and 75% WHC only slight biodegradation was observed (14%). Untreated soil (5% WHC) did not show significant biodegradation ($P > 0.05$). Thus, water content was established as a key factor for biodegradation activity, and 40% WHC was defined as the optimal water content for soil microcosm experiments.

Chemical, microbial, and molecular analyses were carried out on sampling days 0, 21, 45, 90, 135, and 200. At each sampling time, 30 g of soil was extracted as a composite sample from five points in each microcosm and stored at −20°C prior to most analyses; the only exception was microbial counting, which was performed immediately after sampling.

Monitoring the concentrations of total petroleum hydrocarbon and polycyclic aromatic hydrocarbons. Samples were dried for 16 h at room temperature and sieved (<2 mm). Before extraction, an orthoterphenyl acetone solution was added to 2 g of sieved, dried soil as a surrogate internal standard. The spiked sample was extracted five times in an ultrasonic bath (15 min for each extraction) with 10 ml of dichloromethane-acetone (1:1, vol/vol), and the extracts were combined to obtain the total organic extract. The extracts were dried over Na_2SO_4 and concentrated in a rotary evaporator to dryness. The TPH fraction was obtained with an alumina chromatographic column using the EPA3611 method (U.S. Environmental Agency). The TPH fraction and the PAHs were analyzed by gas chromatography with flame ionization detection using a Trace 2000 gas chromatograph (Thermo Quest, Milan, Italy) as described previously (1). Before this, a set of samples was analyzed by gas chromatography with a mass detector to verify the purity of the peaks analyzed by gas chromatography with flame ionization detection (data not shown). Final TPH and PAH concentrations were calculated using standard calibration curves for TPH and each PAH.

Monitoring of heterotrophic and hydrocarbon-degrading microbial populations. Total heterotrophic and PAH-degrading microbial population counts were determined on days 0, 21, 45, 90, 135, and 200 using a miniaturized most-probable-number (MPN) technique as described previously (39).

DNA extraction. Soil samples for DNA extraction were collected from each microcosm on days 0, 21, 45, 90, 135, and 200 in sterile Eppendorf tubes and stored at −20°C prior to analysis.

Total community DNA was extracted from all soil microcosms following a bead beating protocol using an Ultraclean DNA soil extraction kit (MoBio Laboratories, Inc., Solano Beach, CA). Suitable yields of high-molecular-weight DNA (5 to 20 μg g of soil^{-1}) were obtained. An additional purification step with a Clean DNA Wizard kit (Promega, Madison, WI) was employed to avoid PCR inhibition.

Preliminary data for independent triplicate microcosms showed that the Pearson correlation moment vector (r) calculated from the relative band intensities of DGGE profiles for treatments 1M, 2M, and 4M (after 0 and 200 days of incubation) was more than 0.85. These data indicated that there was homogeneity in

TABLE 2. Concentrations and removal of TPH and target PAHs in bioremediation treatments

Compound[c]	Concn (mg kg [dry wt] of soil^{-1})			% Removal from bioremediation treatments at day 200 of incubation				
	Soil, day 0	Dry soil, day 200 (1M)	Autoclaved, day 200 (3M)	40% WHC (2M)	Nutrients (4M)	Biosurfactant (5M)	Inoculated (6M)	Fe octoate (7M)
TPH	8,196 ± 480 A[a]	8,120 ± 285 A	7,570 ± 39 B	79 C	74 D	73 D	73 D	72 D
Acenaphthene	151 ± 4 C	80 ± 7 A	74 ± 2 A	100 B	100 B	100 B	100 B	100 B
Fluorene	182 ± 2 D	137 ± 10 A	117 ± 3 B	100 C	100 C	100 C	100 C	100 C
Phenanthrene	496 ± 24 A	510 ± 23 A	465 ± 10 B	96 C	96 C	97 C	96 C	96 C
Anthracene	114 ± 15 A	85 ± 8 A	95 ± 2 A	84 B	81 B	79 B	80 B	87 B
3C1Phe	72 ± 6 A	75 ± 1 A	71 ± 2 A	100 B	100 B	100 B	100 B	94 B
2C1Phe	78 ± 4 A	81 ± 2 A	78 ± 3 A	100 B	100 B	88 C	83 C	82 C
C1A3	25 ± 5 A	20 ± 1 A	21 ± 1 A	100 B	47 C	44 C	48 C	46 C
CYP4/9C1Phe	131 ± 7 A	128 ± 4 A	116 ± 3 B	97 C	89 C	89 C	89 C	88 C
1C1Phe	40 ± 1 A	41 ± 2 A	40 ± 2 A	100 B	100 B	89 B	100 C	100 B
Fluoranthene	693 ± 48 A	728 ± 38 A	707 ± 33 A	92 B	92 B	94 B	92 B	91 B
Pyrene	387 ± 30 A	403 ± 9 A	386 ± 8 A	87 C	90 C	90 C	89 C	88 C
Benzo(*a*)anthracene	108 ± 10 A	115 ± 3 A	112 ± 4 A	72 B	43 C	40 C	41 C	39 C
Crysene	144 ± 10 A	153 ± 8 A	147 ± 5 A	62 B	39 C	35 C	34 C	33 C
Benzo(*b*+*k*)fluoranthene	82 ± 7 A	71 ± 12 A	80 ± 16 A	0 A	0 A	0 A	0 A	0 A
Benzo(*a*)pyrene	21 ± 2 A	22 ± 1 A	19 ± 1 A	11 A	9 A	0 A	4 A	4 A
Total PAHs[b]	2,724 ± 134 C	2,649 ± 130 C	2,518 ± 148 C	87 A	84 B	83 B	83 B	83 B

[a] Different letters indicate significant differences between treatments ($P < 0.05$).
[b] Total PAHs determined from the total target PAHs analyzed.
[c] 3C1Phe, 3-methyl-phenanthrene; 2C1Phe, 2-methyl-phenanthrene, C1A, methylanthracene; CYP4/9C1Phe, 4-cyclopentaphenanthrene or 9-methyl-phenanthrene; 1C1Phe, 1-methyl-phenanthrene.

each treatment. Hence, DNA was extracted from a composite 0.75-g sample containing 0.25 g of each microcosm replicate.

PCR. The V3 to V5 variable regions of the 16S rRNA gene were amplified using primers 16F341-GC and 16R907 (40). Primer F341-GC included a GC clamp at the 5′ end (5′-CGCCCGCCGCGCCCCGCGCCCGTCCCG CCGCCC CCGCCCG-3′). All PCRs were performed with a personal Mastercycler (Eppendorf, Hamburg, Germany). Fifty microliters of the PCR mixture contained 2.5 U of TaqGold (PE Applied Biosystems, Foster City, CA), 10 mM Tris-HCl (pH 9.0), 50 mM KCl, 1.5 mM $MgCl_2$, each deoxynucleoside triphosphate at a concentration of 200 μM, each primer at a concentration of 0.5 μM, and 100 ng of template DNA quantified by means of the Low DNA Mass Ladder (Gibco BRL, Rockville, MD). After 9 min of initial denaturation at 95°C, a touchdown thermal profile protocol was used, and the annealing temperature was decreased by 1°C per cycle from 65°C to 55°C; then 20 additional cycles at 55°C were performed. Amplification was carried out with 1 min of denaturation at 94°C, 1 min of primer annealing, and 1.5 min of primer extension at 72°C, followed by 10 min of final primer extension. PCRs were done in duplicate using template DNA from soil microcosm composite samples, and then the mixtures were combined prior to DGGE analysis.

DGGE. Approximately 800 ng of purified PCR product quantified by using the Low DNA Mass Ladder (Gibco BRL, Rockville, MD) was loaded onto a 6% (wt/vol) polyacrylamide gel that was 0.75 mm thick (to obtain better resolution), and the denaturing gradients used ranged from 35 to 70% denaturant (100% denaturant contained 7 M urea and 40% formamide). DGGE was performed in 1× TAE buffer (40 mM Tris, 20 mM sodium acetate, 1 mM EDTA; pH 7.4) using a DGGE-2001 system (CBS Scientific Company, Del Mar, CA) at 100 V and 60°C for 16 h.

The gels were stained for 45 min in 1× TAE buffer containing SybrGold (Molecular Probes, Inc., Eugene, OR), viewed under UV light, and analyzed using Image Master (Amersham Pharmacia Biotech, Freiburg, Germany).

Analysis of DGGE images. Images of DGGE gels were digitized, and DGGE bands were processed using the Quantity-one image analysis software (version 4.1; Bio-Rad Laboratories, Hercules, CA) and manually corrected. After normalization of the gels, bands with relative peak area intensities greater than 2% were included in further analyses. Bacterial diversity was assessed using the Shannon-Weaver diversity index (H'), calculated as follows (15): $H' = -\Sigma P_i \log P_i$, where P_i is the relative peak area intensity of a DGGE band, calculated from n_i/N, where n_i is the peak area of the band and N is the sum of all peak areas in the densitometry curve. Furthermore, a covariance principal-component analysis (PCA) of band types and peak heights was carried out for treatments 1M, 2M, and 4M to consider possible shifts in the composition of the microbial populations. The effect of bioaugmentation (treatment 6M) on the microbial diversity of the soil was assessed by comparing the DGGE profiles for treatments 1M (untreated), 4M (nutrients added), and 6M (nutrients and inoculum added) by a similarity cluster analysis. A dendrogram was constructed using the unweighted pair group method with the Pearson product-moment correlation coefficient calculated from the complete densitometric curves for fingerprints of soil bacterial community microcosms. The PCA and similarity cluster analysis were performed using the Excel application StatistiXL, version 1.4.

Sequencing and phylogenetic analysis of denaturing gradient gel electrophoresis bands. Predominant DGGE bands were excised with a sterile razor blade, resuspended in 50 μl sterilized MilliQ water, stored at 4°C overnight, reamplified, cloned in the pGEM-T Easy vector (Promega, Madison, WI), and sequenced by using an ABI Prism Big Dye terminator cycle sequencing reaction kit, version 3.1 (Perkin-Elmer Applied Biosystems, Foster City, CA), and an ABI 3700 DNA sequencer (Perkin-Elmer Applied Biosystems, Foster City, CA) and following the manufacturer's instructions.

Sequences were edited and assembled using version 4.8.7 of the BioEdit software (17), inspected for the presence of ambiguous base assignments, and subjected to the Check Chimera program of the Ribosomal Database Project (24) before the sequences were examined with the BLAST and RDP search alignment tool comparison software (4, 24).

Statistical analysis. Data were subjected to analysis of variance using the Statgraphics Plus package (version 5.1; Statistical Graphics Corp., Manguistics Inc., United States). Duncan's multiple-range test of means, with a significance level of 0.05, was applied to the results to determine their statistical significance.

Nucleotide sequence accession numbers. The 38 nucleotide sequences identified in this study have been deposited in the GenBank database under accession numbers AY58562 to AY758599.

RESULTS

Soil properties. The soil was a loamy clay soil containing 40% clay, 28% silt, and 32% sand. The total organic carbon and total nitrogen contents were 4.2% and 0.15%, respectively; the inorganic nitrogen content was 20 mg kg^{-1} nitrate and 2.8 mg kg^{-1} ammonium, and the phosphate content was low (less than 1 mg kg^{-1}). The soil had low conductivity (228 μS cm^{-2}), the pH was 7,5, and the water content was extremely low (1.6%). Conversely, the soil had a high WHC (27.7%), possibly due to the high clay content. The PAH degraders accounted for up to 12% of the total heterotrophic microbial population, with 1.8×10^5 cells g (dry weight) of $soil^{-1}$.

Total petroleum hydrocarbon and polycyclic aromatic hydrocarbon biodegradation. The contaminated soil had a high initial TPH concentration (around 8,000 mg kg [dry weight] of soil^{-1}) (Table 2). When aromatic compounds were examined, no phenol derivatives, naphthalene, or alkyl derivatives of naphthalene were detected (the detection limit was more than 0.5 μg g [dry weight] of soil^{-1}). Consequently, we presumed that a limited amount of PAHs and TPH was lost by evaporation and/or biodegradation prior to soil sampling. PAHs with three and four rings were the most abundant components, and their concentrations were between 100 and 700 mg kg^{-1}. The polyaromatic fraction accounted for 90% of the TPH fraction (as determined by gravimetric measurement), while the TPH accounted for 85% of the total organic extract.

The TPH concentration did not decrease significantly ($P > 0.05$) in the untreated soil (treatment 1M) over the course of the 200-day experiment, whereas there was a slight decrease in autoclaved soil (treatment 3M). The same behavior was observed for the target PAHs. Hence, untreated dry soil (treatment 1M) was used as a control with which to calculate hydrocarbon biodegradation for the different treatments and to compare changes in microbial diversity.

By the end of the experiment (200 days), significant TPH biodegradation was observed for all treatments (treatments 2M and 4M to 7M) (Table 2). Biostimulation without nutrient addition (treatment 2M) resulted in slightly greater TPH depletion ($P < 0.05$) than the treatments in which nutrients were added (treatments 4M to 7M).

To study the rates of biodegradation of TPH and target PAHs, biphasic TPH degradation kinetics were assessed because a single first-order decay curve fitted to the entire data set did not adequately explain ($r^2 < 0.8$) the changes in TPH concentration observed during the course of the experiment. Thus, two degradation rates (k_1 and k_2) were defined according to the breakpoints that best fit the data for all treatments; k_1 was used for the early-stage group (from 0 to 45 days of incubation), and k_2 was used for the late-stage group (from 90 to 200 days of incubation) (Table 3). It is important to note that k_2 was 1 order of magnitude lower than k_1 for all treatments, with values near zero for treatments with nutrients. During the first 45 days, the first-order TPH degradation rate constant (k_1) was slightly lower for the treatment without nutrients (treatment 2M) than for the other treatments. In contrast, the rate constant (k_2) for the late stage (90 to 200 days) was higher ($P < 0.05$). These rate constants are similar to those reported in other studies of bioremediation in hydrocarbon-contaminated soils (18, 35).

Two- and three-ring PAHs were highly degraded (80 to 100%) during the first 45 days, and the biodegradation rate (k) was the same for all treatments ($P > 0.05$) (Tables 2 and 3). An exception was 1-methyl-anthracene, for which the biodegradation rate was higher ($P < 0.05$) in treatments without nutrient amendment. Interestingly, phenanthrene and anthracene were not completely degraded (Table 2). One possible explanation for this could be the low bioavailability of the residual quantities of these compounds present after day 45 (31). The biodegradation kinetics of fluoranthene were not affected by nutrient addition (Table 3), whereas the early-stage biodegradation kinetics (k_1) of pyrene were slower in the absence of nutrient addition ($P < 0.05$).

TABLE 3. First-order biodegradation rates of TPH and target PAHs during the bioremediation experiment

Treatment[a]	Biodegradation rates (day^{-1})[b]													
	TPH		Acenaphthene	Fluorene	Phenanthrene	Anthracene	Fluoranthene		Pyrene		Benzo(*a*)anthracene		Chrysene	
	k_1	k_2	k	k	k	k	k_1	k_2	k_1	k_2	k_1	k_2	k_1	k_2
2M (no nutrients)	−0.0200 A[c]	−0.0039 A	−0.0133 A	−0.1240 A	−0.1107 A	−0.0264 A	−0.0258 A	−0.0067 A	−0.0089 A	−0.0067 A	−0.0111 A	−0.0043 A	−0.0062 A	−0.0041 A
4M (nutrients)	−0.0245 B	−0.0019 B	−0.0113 A	−0.1412 A	−0.1269 A	−0.0265 A	−0.0283 A	−0.0048 A	−0.0223 B	−0.0041 A	−0.0103 A	−0.0002 B	−0.0102 B	−0.0017 B
5M (nutrients + biosurfactant)	−0.0269 C	−0.0008 B	−0.0157 A	−0.1406 A	−0.1261 A	−0.0265 A	−0.0339 B	−0.0048 A	−0.0265 B	−0.0062 A	−0.0117 A	−0.0008 B	−0.0111 B	−0.0004 B
6M (nutrients + inoculum)	−0.0244 B	−0.0010 B	−0.0124 A	−0.1373 A	−0.1252 A	−0.0236 A	−0.0334 B	−0.0068 A	−0.0252 B	−0.0059 A	−0.0092 A	−0.0008 B	−0.0100 B	−0.0016 B
7M (nutrients + Fe octoate)	−0.0237 B	−0.0006 B	−0.0124 A	−0.0965 A	−0.0923 A	−0.0254 A	−0.0297 A	−0.0057 A	−0.0217 B	−0.0063 A	−0.0093 A	−0.0008 B	−0.0092 B	−0.0007 B

[a] All treatments were carried out with triplicate independent samples at 40% water holding capacity.

[b] Acenaphthene, fluorene, and phenanthrene were highly degraded during the first 21 days. Their k values are values for the entire incubation time ($r > 0.95$). k, 0 to 200 days of incubation; k_1, 0 to 45 days of incubation; k_2, 90 to 200 days of incubation.

[c] Different letters within columns indicate that there are significant differences in biodegradation rates between treatments ($P < 0.05$).

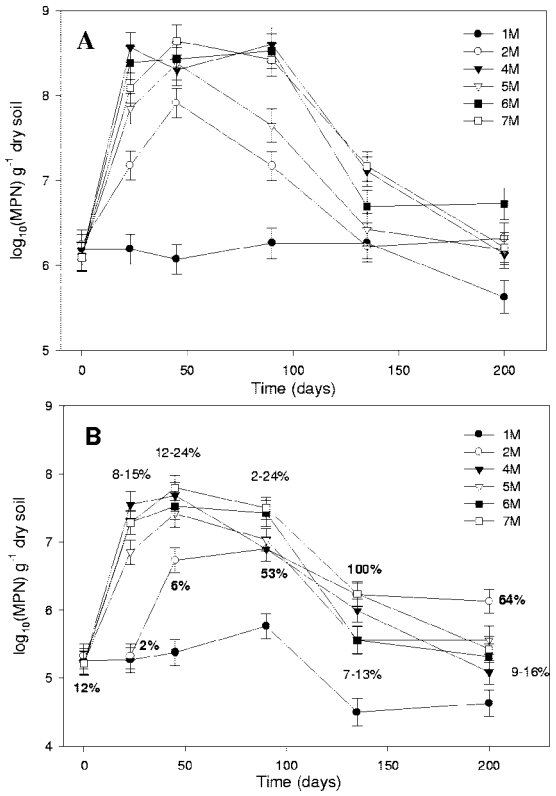

FIG. 1. Heterotrophic (A) and PAH-degrading (B) populations in soil treatments over the course of 200 days of incubation. Autoclaved soil (treatment 3M) presented a microbial population only after 135 days of incubation (10 to 100 MPN g [dry weight] of soil^{-1}) (data not shown). The values in boldface type are percentages for the PAH-degrading population for the basic treatment (treatment 2M), whereas the other values are values for the PAH-degrading populations for the nutrient treatments and untreated soil.

The degree of benzo(*a*)anthracene and chrysene degradation was significantly different when biostimulation without addition of nutrients (treatment 2M) was compared with treatments in which nutrients were added (treatments 4M to 7M). Both compounds were degraded more ($P < 0.05$) under biostimulation conditions without nutrient addition than in treatments with nutrient addition (Table 2). Furthermore, the late-stage biodegradation rates were significantly higher ($P < 0.05$) without nutrient addition [10-fold higher for benzo(*a*)anthracene biodegradation and threefold higher for chrysene biodegradation] (Table 3). Benzo(*a*)pyrene and benzo(*b*+*k*)fluoranthene were not significantly degraded ($P > 0.05$). The percentages of PAH biodegradation and the kinetics are similar to those reported in other studies (7, 12).

Monitoring of the heterotrophic and polycyclic aromatic hydrocarbon-degrading microbial populations. As shown in Fig. 1, the sizes of both the heterotrophic and PAH-degrading microbial populations increased 2 to 3 orders of magnitude between day 0 and day 21 for treatments in which there was nutrient addition (treatments 4M to 7M), whereas the population subjected to the biostimulation treatment without nutrient addition (treatment 2M) increased more slowly (1 to 2 orders of magnitude at 21 to 45 days). After 90 days of incubation, the sizes of both populations returned to the initial values for treatments in which there was nutrient addition (treatments 4M to 7M), whereas for treatment 2M the PAH-degrading population remained 1 order of magnitude larger than the population at the initial stage. In untreated dry soil (treatment 1M), the size of the heterotrophic population remained constant until day 135 and the size of the PAH-degrading population remained constant until day 90. Between days 135 and 200 the sizes of the two populations decreased by approximately 1 order of magnitude.

Aeration and the optimal humidity (treatment 2M) resulted in a remarkable shift in the proportion of the PAH-degrading population (Fig. 1).

No differences in microbial population counts were observed when the results for addition of biosurfactant (treatment 5M), addition of ferric octoate (treatment 7M), or bioaugmentation (treatment 6M) were compared with the results for treatment 4M.

Analysis of treatments by denaturing gradient gel electrophoresis. The biodegradation results and microbial counts revealed three different treatment groups: (i) untreated soil, (ii) treated soil without nutrient addition, and (iii) treated soil with nutrient addition. Thus, the effects of different biostimulation conditions on the structure and dynamics of the bacterial community were analyzed by DGGE by using samples from treatments 1M (untreated soil), 2M (aerated soil at 40% water-holding capacity without nutrient addition), and 4M (like treatment 2M but with nutrient addition) taken during the 200-day experiment. In addition, the effect of bioaugmentation (treatment 6M) was monitored by DGGE, and this treatment was compared with treatments 4M and 1M.

The bacterial community in untreated soil (treatment 1M) was complex (27 or 28 DGGE bands) and did not change over the course of the 200-day experiment (Fig. 2). However, biostimulation treatments with (treatment 4M) and without (treatment 2M) nutrient addition resulted in shifts in the composition of the microbial community. In particular, the initial profiles (21 and 45 days) were clearly different; the 2M and 4M treatments produced 22 to 24 and 19 to 22 DGGE bands, respectively (Fig. 2).

The microbial diversity decreased during the maximum biodegradation period for all treatments, from 1.28 on day 0 to 1.18 after 90 days, and remained low until the end of the incubation. Other authors have described both increases and reductions in diversity during biodegradation. Our results are similar to those reported by Andreoni et al. (6) obtained with a PAH-contaminated soil, whereas Kaplan and Kitts (18) and Zucchi et al. (41) reported increases in diversity during bioremediation of crude oil-contaminated soil.

Principal-component analysis of the bacterial community. Temporal changes in the bacterial community were monitored using principal-component analysis (Fig. 3). Based on visual inspection of the raw data, there was a clear difference in the DGGE profiles between microcosms that depended on the time and type of biostimulation treatment. PCA revealed three different groups; the first group consisted of untreated soil (at 0 and 200 days), and the second and third groups consisted of biostimulated soil with and without nutrient addition, respectively. Both biostimulation treatments (treatments 2M and 4M) exhibited a noticeable and regular separation from untreated soil (treatment 1M) in the first principal component (PC1), which explained 35.9% of the variation in the data

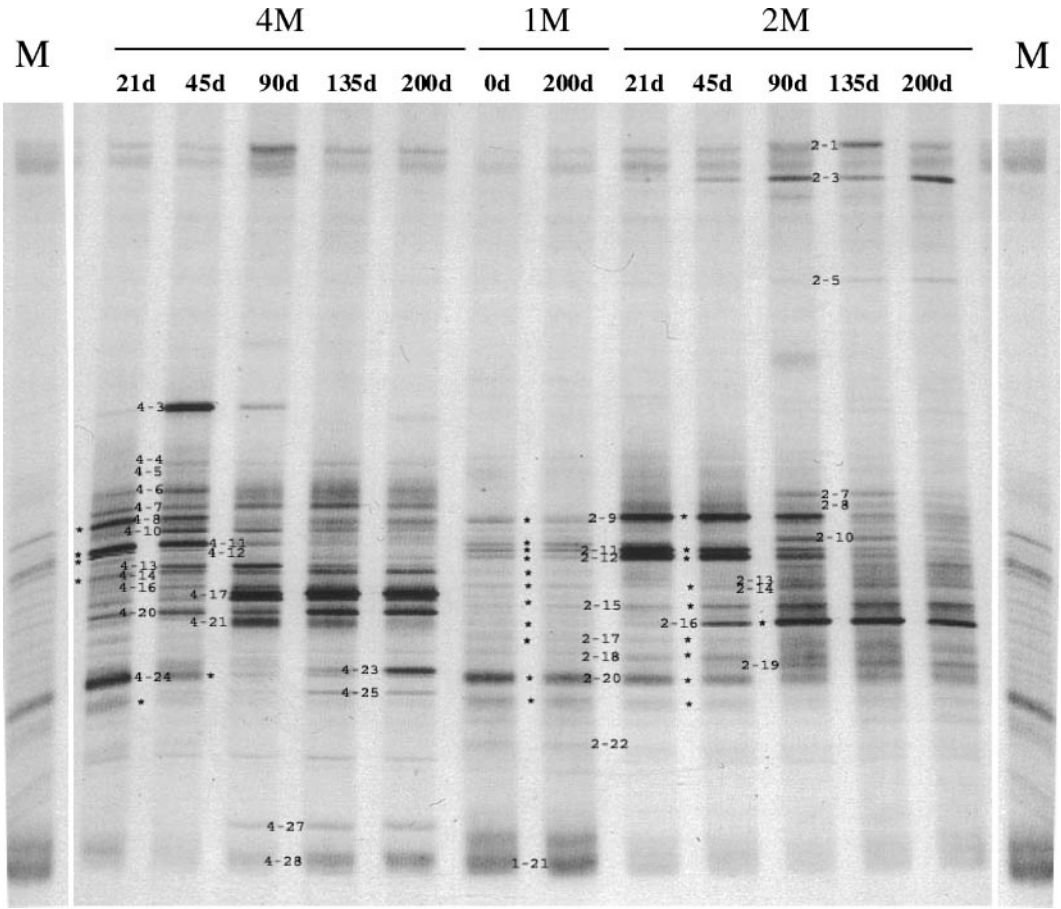

FIG. 2. Denaturing gradient gel electrophoresis (35 to 70% denaturant) of PCR-amplified 16S rRNA gene fragments from treatments 4M (with nutrient addition), 1M (untreated dry soil), and 2M (without nutrient addition) over the course of a of 200-day incubation. Lane M contained a DNA soil sample (treatment 1M) obtained at 200 days that was used as a marker. The asterisks indicate comigration with bands from untreated soil.

during the 200 days of incubation (Fig. 3). Furthermore, for each treatment the PC1 value was increasingly far from the initial point as incubation time increased. The highest second principal component (PC2) for the 2M treatment corresponded to positive values, while for the 4M treatment the values were negative (Table 4). This could explain the distance in PC2 observed between the biostimulation treatments. Analysis of variance of the PC2 scores, which represented 24.0% of the variation in the data, showed that there was a significant difference between biostimulation groups ($P < 0.05$) over the course of the experiment. Coincidentally, the greatest change in PC2 occurred during the first 45 days of incubation, during which the TPH biodegradation rates were more significant (Table 2).

It is interesting that only two bands were shared by different treatments. Bands B2-11 and B2-20 were identical to bands B4-12 and B4-24, respectively. Furthermore, these DGGE bands displayed similar dynamics for the two treatments and exhibited the most negative PC1 loading values (0.909 and 0.961, respectively). Their dynamics could explain the migration along PC1 observed for both treatments. The treatment 2M bands with the highest PC2 loading values were B2-3 and B2-16, while for the 4M treatment B4-17 had the most negative

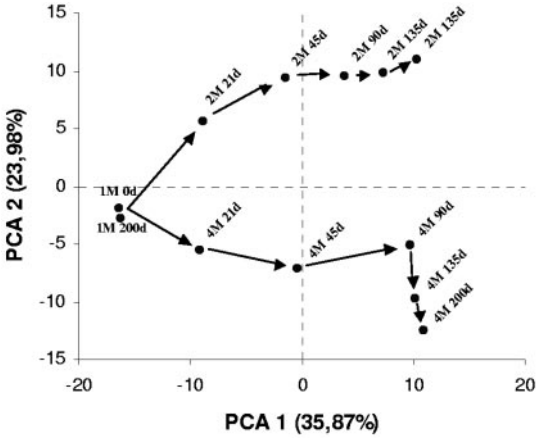

FIG. 3. Principal-component analysis scatter plot of denaturing gradient gel electrophoresis profiles (Fig. 2) over the course of the incubation period. 1M, 2M, and 4M indicate untreated soil (dry soil), aerated soil at 40% WHC without nutrient addition, and aerated soil at 40% WHC with nutrient addition, respectively. The numbers of days after treatment are also indicated; for example, 4M 135d indicates biostimulated soil with nutrient addition on day 135.

TABLE 4. Properties of bands from DGGE: designations and accession numbers for the band sequences and levels of similarity to related organisms

DGGE band[e]	Accession no.	PCA loading		% Similarity[a]	Closest organism in GenBank database (accession no.)	Phylogenetic group[b]
		PC1	PC2			
No nutrients (2M)[c]						
B2-1 (135–200 days)[d]	AY758563	0.490	0.248	98.4	*Sphingomonas yanoikuyae* Q1 (SY37525)	*Sphingomonadaceae* (α)
B2-3 (90–200 days)	AY758564	0.390	0.826	97.7	Enyironmental CEB clone (AY038771)	*Sphingobacteriales* (CFB group)
B2-5	AY758565	−0.012	0.596	95.4	*Cytophaga* sp. strain MDA2507 (AY238333)	*Flavobacteriaceae* (CFB group)
B2-7	AY758566	0.565	−0.458	96.7	Uncultured bacterium (AF465658)	Unclassified γ-*Proteobacteria*
B2-8 (21–45 days)	AY758567	0.399	−0.297	98.5	*Acidovorax* sp. strain UFZ-B517 (AF235010)	*Comamonadaceae* (β)
B2-9* (21–90 days)	AY758568	−0.407	0.299	97.1	*Xanthomonas axonopodis* (AF442742)	*Xanthomonadaceae* (γ)
B2-11* (21–90 days)	AY758569	−0.909	0.337	96.7	Environmental clone (AJ318120)	*Sphingomonadaceae* (α)
B2-12* (21–90 days)	AY758570	−0.477	0.643	98.4	*Sphingomonas* sp. strain CFO6 (SC52146)	*Sphingomonadaceae* (α)
B2-13	AY758571	0.189	0.531	96.4	*Sphingomonas* sp. strain JSI (SSP427917)	*Sphingomonadaceae* (α)
B2-14*	AY758572	0.189	0.531	98.6	Environmental clone AP-16 (AY145553)	*Rhizobiales* (α)
B2-15* (45–200 days)	AY758573	0.882	−0.186	94.5	Environmental clone (AB074615)	*Xanthomonadaceae* (γ)
B2-16* (45–200 days)	AY758574	0.646	0.644	99.6	Environmental clone (AB074615)	*Xanthomonadaceae* (γ)
B2-17*	AY758575	−0.813	−0.064	99.8	Environmental clone (AY133099)	*Rhodospirillaceae* (α)
B2-18*	AY758576	−0.058	−0.657	96.3	*Sphingomonas* sp. (X72723)	*Sphingomonadaceae* (α)
B2-19 (90–200 days)	AY758577	0.630	−0.199	97.2	Environmental clone C5-K12 (UBA421218)	Unclassified γ-*Proteobacteria*
B2-20* (21–45 days)	AY758578	−0.961	0.100	99.8	*Azospirillum* clone GCPF30 (AY129799)	*Rhodospirillaceae* (α)
B2-22	AY758579	−0.166	0.547	97.3	*Roseomonas* genomospecies (AY150048)	*Rhodospirillales* (α)
Nutrient addition (4M)						
B4-3 (45 days)	AY758580	0.097	−0.278	100	*Sphingomonas* sp. strain S37 (AF367204)	*Sphingomonodaceae* (α)
B4-4	AY758581	0.643	−0.538	94.7	*Brevandimonas alba* H12C5 (AF296688)	Unclassified α-*Proteobacteria*
B4-5	AY758582	−0.675	0.337	99.4	*Trojanella thessalonices* (AF069496)	*Rhodospirillaceae* (α)
B4-6 (21–45 days)	AY758583	0.565	−0.458	98.5	*Agrobacterium tumefaciens* (ATU295683)	*Rhizobiaceae* (α)
B4-7 (21 days, 90–200 days)	AY758584	0.399	−0.297	97.5	*Alcaligenes* sp. (ASP16SRRN)	*Alcaligenaceae* (β)
B4-8* (21–45 days)	AY758585	−0.407	0.299	98.9	*Xanthomonas* sp. strain V4.BO.41 (AJ244722)	*Xanthomonadaceae* (γ)
B4-10 (45–135 days)	AY758586	0.342	−0.667	93.9	Environmental clone (AJ532712)	Unclassified γ-*Proteobacteria*
B4-11* (21–45 days)	AY758587	−0.597	−0.559	99.8	*Sphingomonas herbicidovorans* (AB022428)	*Sphingomonadaceae* (α)
				99.2	*Sphingomonas paucimobilis* EPA505(X94100)	
B4-12* (21–45 days)	AY758588	−0.909	0.337	95.3	*Sphingomonas adhaesiva* (SA16SRD3)	*Sphingomonadaceae* (α)
B4-13 (45–90 days)	AY758589	0.435	0.003	92.7	*Erythrobacter* sp. (AB011075)	*Sphingomonadaceae* (α)
B4-14* (135–200 days)	AY758590	0.263	−0.669	95.1	*Xanthomonas* sp. strain V4.BO.41 (AJ244722)	*Xanthomonadaceae* (γ)
B4-16 (90 days)	AY758591	0.189	0.531	99.8	*Achromobacter xylosoxidans* (AF225979)	*Alcaligenaceae* (β)
B4-17 (90–200 days)	AY758592	0.519	−0.787	95.0	*Xanthomonas* sp. strain V4.BO.41 (AJ244722)	*Xanthomonadaceae* (γ)
B4-20 (21–200 days)	AY758593	0.882	−0.186	98.8	*Achromobacter* sp. strain LMG5911 (AY170848)	*Alcaligenaceae* (β)
B4-21 (90–135 days)	AY758594	0.646	0.644	96.3	*Xanthomonas* sp. strain V4.BO.41 (AJ244722)	*Xanthomonadaceae* (γ)
B4-23 (135–200 days)	AY758595	0.630	−0.199	97.8	*Sinorhizobium frediii* USDA257 (AY260150)	*Rhizobiaceae* (α)
B4-24* (21–45 days)	AY758596	−0.961	0.100	99.8	*Azospirillum* clone GCPF30 (AY129799)	*Rhodospirillaceae* (α)
B4-25	AY758597	0.514	−0.679	90.1	*Erytrobacter* sp. strain AS-45 (ESP391206)	*Sphingomonadaceae* (α)
B4-27	AY758598	0.586	−0.666	93.2	*Roseomonas* genomospecies strain ATCC 49961 (AY150050)	*Rhodospirillaceae* (α)
B4-28 (135–200 days)	AY758599	−0.612	−0.340	96.6	*Rhodococus* sp. strain RHA6 (RS16316)	*Nocardiaceae* (high-G+C-content gram-positive bacteria)

[a] Sequences were matched with the closest relative from the GenBank database.
[b] Sequences were matched with the closest relative from the Ribosomal Database Project (40). α, β, and γ, α-, β-, and γ-*Proteobacteria*, respectively.
[c] Treatments without nutrients (2M) and with nutrient addition (4M) were carried out at 40% water-holding capacity in aerated soils by mixing twice a week.
[d] The incubation days with relative area intensity greater than 5% are indicated in parentheses. The relative intensity was calculated by avoiding background noise from the DGGE gel (Fig. 3) with Quantity-one 4.4.1 software (Bio-Rad, Hercules, CA).
[e] Asterisks indicate comigrating bands with untreated soil (treatment 1M).

PC2 loading value. Band B4-3, which was the most abundant band in the early biodegradation stage at 0 to 45 days for the 4M treatment, disappeared after 90 days and did not have a high PCA loading value (Table 4). Nevertheless, this band could be important in the biodegradation of three-ring PAHs because at this time these compounds exhibited maximum depletion.

Phylogenetic and dynamic analysis of excised bands. Taxonomic assignments of the prominent DGGE bands were determined for biostimulation treatments 2M and 4M. Bands from untreated soil (treatment 1M) were not excised because they were weak, but they were assigned to comigrating bands of treatments 2M and 4M which exhibited higher intensity (Fig. 2 and Table 4). Table 4 shows the closest relatives of DGGE bands excised for biostimulation treatments 2M and 4M. Most of the sequences derived from DGGE bands exhibited levels of similarity greater than 95%.

Taking into account the assignment to comigrating bands, the original soil contained five α-*Proteobacteria* (*Sphingomonas*, *Rhizobium-Agrobacterium*, and *Azospirillum* groups) and eight γ-*Proteobacteria* (*Xanthomonas* group), according to RDP classification (24). Biostimulated soil from treatment 2M

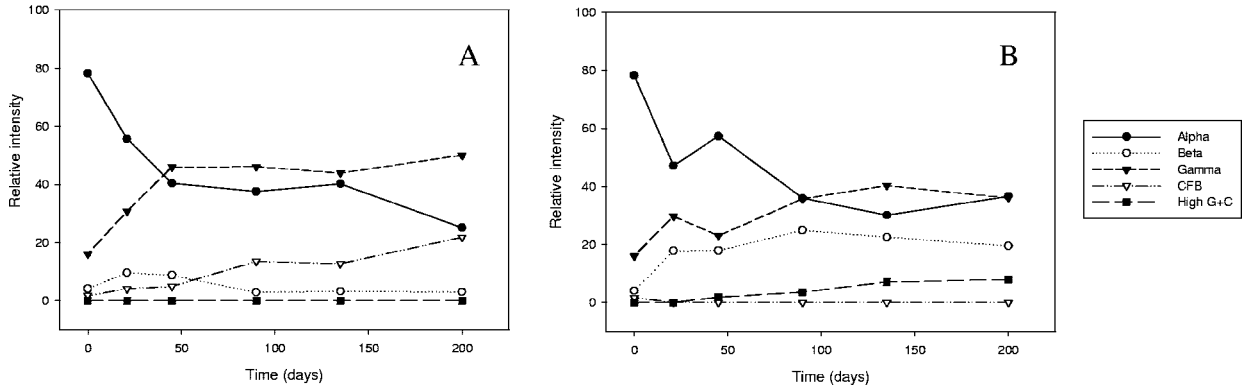

FIG. 4. Phylogenetic groups during the bioremediation experiment. (A) Treatment 2M (biostimulation without nutrient amendment). (B) Treatment 4M (biostimulation with nutrient amendment). Excised bands from treatment 2M accounted for 73 to 84% of the total lane intensity, whereas for treatment 4M excised bands accounted for 81 to 91% of the total band intensity. On day 0, the bands studied account for 70% of the total signal of the lane. Alpha, α-*Proteobacteria*; Beta, β-*Proteobacteria*; Gamma, γ-*Proteobacteria*; CFB, *Cytophaga-Flexibacter-Bacteroides* group; High G+C, high-G+C-content gram-positive bacteria.

contained 53% α-*Proteobacteria* (9/17 DGGE bands), 6% β-*Proteobacteria* (1/17 DGGE bands), and 23% γ-*Proteobacteria* (4/17 DGGE bands) (Table 4). No rhodococci were found, but the closest relatives to the *Cytophaga-Flavobacterium-Bacteroides* (CFB) group, which accounted for 12% of the sample (2/17 DGGE bands), were found after 45 days. Soil subjected to the 4M treatment contained 55% α-*Proteobacteria* (11/20 DGGE bands), 15% β-*Proteobacteria* (3/20 DGGE bands), 25% γ-*Proteobacteria* (5/20 DGGE bands), and 5% high-G+C-content gram-positive bacteria (1/20 DGGE bands). No close relatives belonging to the CFB group were found in the 4M treatment soil.

At early stages (0 to 90 days), for treatment 2M soil five dominant bands (relative intensity greater than 5%) were observed (B2-11, B2-12, B2-20, B2-8, and B2-9) (Table 4). Three of these bands (B2-11, B2-12, and B2-20) belonged to α-*Proteobacteria (Sphingomonadaceae* and *Rhodospirillaceae)*, whereas B2-8 belonged to β-*Proteobacteria (Comamonadaceae*) and B2-9 belonged to γ-*Proteobacteria* (*Xanthomonadaceae*). Neither CFB bacteria nor high-G+C-content gram-positive bacteria were found at early stages of biodegradation.

At late stages (90 to 200 days), for treatment 2M soil five dominant bands (relative intensity greater than 5%) were observed (B2-1, B2-3, B2-15, B2-16, and B2-19) (Table 4). Three of these bands (B2-15, B2-16, and B2-19) belonged to the γ-*Proteobacteria (Comamonadaceae* and *Xanthomonadaceae*). B2-1 belonged to the α-*Proteobacteria* (*Sphingomonadaceae*), and B2-3 belonged to the CFB group (*Crenotrichaceae*). Neither β-*Proteobacteria* nor high-G+C-content gram-positive bacteria were found.

At early stages (0 to 90 days), for treatment 4M soil nine dominant bands (relative intensity greater than 5%) were observed (B4-3, B4-6, B4-8, B4-10, B4-11, B4-12, B4-13, B4-20, and B4-24) (Table 4). Six of these bands (B4-3, B4-6, B4-11, B4-12, B4-13, and B4-24) belonged to α-*Proteobacteria (Sphingomonadaceae*, *Rhizobiaceae*, and *Rhodospirillaceae*), one band (B4-20) belonged to β-*Proteobacteria* (*Alcaligenaceae*), and two bands (B4-8 and B4-10) belonged to γ-*Proteobacteria* (*Xanthomonadaceae*). Neither CFB bacteria nor high-G+C-content gram-positive bacteria were found.

At late stages (90 to 200 days), for treatment 4M soil nine dominant bands (relative intensity greater than 5%) were observed (B4-7, B4-10, B4-14, B4-17, B4-20, B4-21, B4-23, and B4-28). Four of these bands (B4-10, B4-14, B4-17, and B4-21) belonged to γ-*Proteobacteria* (*Xanthomonadaceae* and unclassified group), two bands (B4-20 and B4-7) belonged to β-*Proteobacteria* (*Alcaligenaceae*), and one band (B4-23) belonged to α-*Proteobacteria* (*Rhizobiaceae*), whereas band B4-28 belonged to the high-G+C-content gram-positive bacteria (*Nocardiaceae*). No CFB bacteria were found.

Phylogenetic groups during bioremediation. At the beginning of the experiment, α-*Proteobacteria* (78%), dominated by *Sphingomonadaceae*, were predominant in contaminated soil, followed by γ-*Proteobacteria* (16%), dominated by *Xanthomonadaceae*, whereas the other groups were scarce. During biodegradation, the microbial population shifted dramatically, and after 200 days of incubation of the 2M treatment, γ-*Proteobacteria* were dominant (50%), followed by α-*Proteobacteria* (25%) and the CFB group (22%), while for the 4M treatment, α-*Proteobacteria* and γ-*Proteobacteria* were the dominant groups (36% each), followed by β-*Proteobacteria* and high-G+C-content gram-positive bacteria (19% and 8%, respectively) (Fig. 4).

A correlation analysis of the phylogenetic groups and evolution of the TPH concentration showed that the α- and γ-*Proteobacteria* exhibited the highest positive and inverse correlations with the TPH concentration, respectively (r^2 = 0.92 to 0.93) for the 2M treatment; for the 4M treatment the α-*Proteobacteria* exhibited the highest positive correlation (r^2 = 0.78), whereas the β-*Proteobacteria* exhibited the highest inverse correlation (r^2 = 0.85), followed by the γ-*Proteobacteria* (r^2 = 0.78). For target PAH concentrations in the 2M treatment, the CFB group exhibited the highest inverse correlation (r^2 = 0.81 to 0.85) with the pyrene, benzo(*a*)anthracene, and chrysene concentrations, whereas α-*Proteobacteria* and γ-*Proteobacteria* exhibited the highest positive and inverse correlations with fluoranthene (r^2 = 0.92 to 0.94), phenanthrene (r^2 = 0.76), and anthracene (r^2 = 0.84). β-*Proteobacteria* did not exhibit good correlations with target PAHs (r^2 = 0 to 0.4). In contrast, for nutrient treatment 4M, α-*Proteobacteria* and β-*Proteobacteria* exhibited the highest positive and inverse cor-

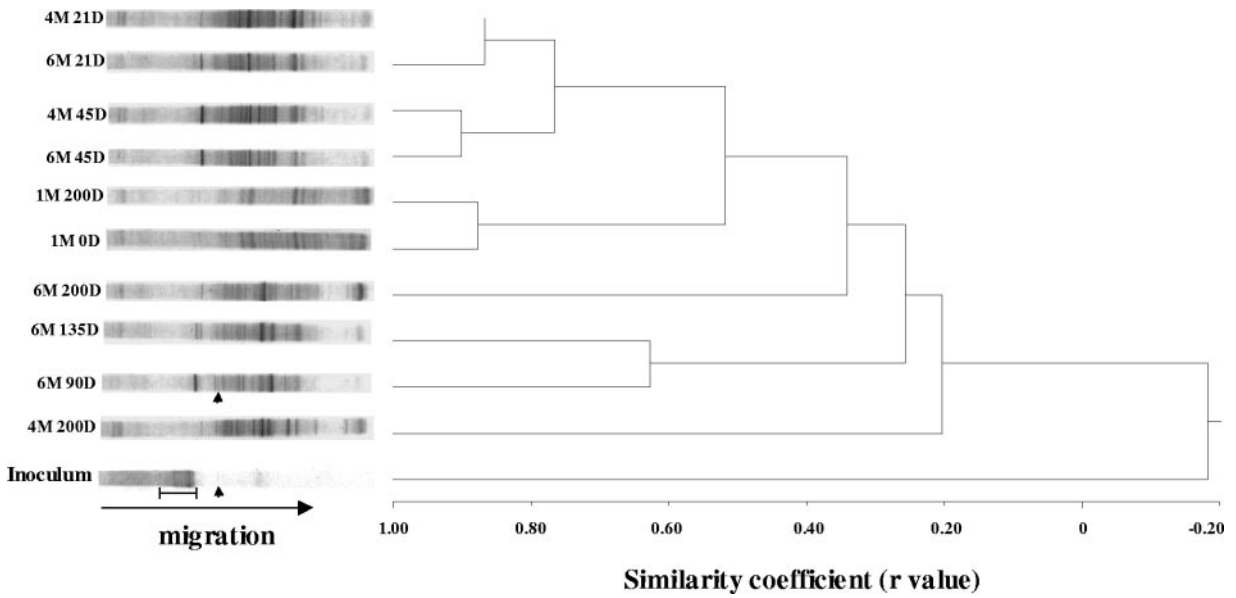

FIG. 5. Denaturing gradient gel electrophoresis profile and cluster analysis (Pearson product moment, unweighted pair group method) for the bioaugmentation treatment (treatment 6M), the nutrient addition treatment (treatment 4M), and untreated dry soil (treatment 1M) over the course of 200 days of incubation. The codes on the left indicate the treatment and the number of days of incubation; for example, 6M 21D indicates treatment 6M and incubation for 21 days. The cross-hatched area in the inoculum lane shows major bands that did not comigrate. The arrows indicate the only band that comigrated for the inoculum and the bioaugmented soil.

relations, respectively, with fluoranthene and pyrene ($r^2 = 0.83$ to 0.89). Also, β-*Proteobacteria* exhibited a good inverse correlation with phenanthrene, anthracene, benzo(*a*)anthracene, and chrysene ($r^2 = 0.84$ to 0.92). γ-*Proteobacteria* exhibited lower correlations with PAH concentrations ($r^2 = 0.5$ to 0.7) for the 4M treatment.

Monitoring bioaugmentation by denaturing gradient gel electrophoresis. At the beginning of the experiment, the profiles for biostimulation and bioaugmentation were very similar, forming two clusters (21 and 45 days) in each of the two treatments (Fig. 5). Only one of the DGGE bands from the inoculum was shared in inoculated soil during the 200 days of the experiment. Taking into account the fact that inoculation was performed five times (days 14, 26, 57, 120, and 165) in order to have 10^8 microorganisms g (dry weight) of soil^{-1} at each time of addition, this result implies that the inoculum did not compete favorably with the indigenous bacterial community during the first stages of PAH biodegradation. However, at 200 days the DGGE profiles for biostimulation and bioaugmentation were quite different. Hence, it seems that at early stages, when the biodegradation process was dominant, an exogenous inoculum did not affect the distribution of the indigenous microbial population, while at late stages, when the biodegradation of PAHs and TPH was very slow, it could have an effect (Table 2).

DISCUSSION

A creosote-contaminated soil from a wood treatment facility that had been operating for at least 30 years was the subject of the present study. A high proportion of PAH-degrading bacteria at the beginning of the experiment (Fig. 1) and the absence of a lag phase at the beginning of TPH degradation (data not shown) revealed the presence of a preadapted PAH-degrading microbial population in the original soil.

Effects of different treatments on the degradation of polycyclic aromatic hydrocarbons. The kinetics of TPH degradation displayed a biphasic pattern for all bioremediation treatments. This behavior may have been due to a number of factors, such as a decrease in PAH bioavailability (3), accumulation of toxic PAH metabolites (11), or enrichment of more recalcitrant compounds (30). In a parallel study, a decrease in bioavailability was demonstrated (31). The accumulation of metabolites resulting from oxidation of PAHs can reduce the viability of several PAH degraders in addition to inhibiting the degradation of PAH (11, 20, 21). Nevertheless, this probably was not the case in this study, because polar metabolites determined by gas chromatography-mass spectrometry of the derivatized polar fraction did not accumulate in the soil (31). In addition, leachates from the soil after the different treatments showed that there was a reduction in soil toxicity, as determined by Microtox (31).

Taking into account the finding that in the original dry soil (water content, 1.6%) the TPH concentration was not reduced during the experiment, water content and aeration became the key factors for soil bioremediation. The quantities of nutrients added in our treatments, taking into account only the inorganic nitrogen forms, were established in order to obtain a molar C/N/P ratio of 300:10:1. The required quantities were added at three times during the experiment in order to avoid inhibition caused by a drastic osmotic change, as has been described elsewhere (38). Recently, Atagana (7) described the ratio used in this study as optimal for a creosote-contaminated soil.

As shown in Table 3, our results suggest that nutrient addition had a negative effect on late-stage biodegradation of four-ring PAHs and TPHs. The presence of an excess of nutrients

could have inhibited the biodegradation of high-molecular-weight PAHs. In fact, Rhykerd et al. (27) described a reduction in bioremediation of a motor oil due to an increase in the salinity produced by NaCl, and Braddock et al. (10) attributed a reduction in the microbial activity of an Arctic hydrocarbon-contaminated soil to the salinity produced by an excess of nutrients.

In a recent study, Roling-Wilfred et al. (29) suggested that the addition of nutrients implies that there are differences in hydrocarbon biodegradation rates and variations in the microbial population. Therefore, for the present study, the differential microbial population shifts due to different inorganic nutrient contents may also explain the different biodegradation capabilities observed for biostimulation treatments with and without nutrient addition.

Response of the microbial population to bioremediation of polycyclic aromatic hydrocarbons. At early stages (0 to 45 days) of the bioremediation process, the addition of nutrients caused significant increases in both the heterotrophic and PAH-degrading microbial populations, while soil stimulated only by aeration and optimum humidity exhibited smaller increases in the sizes of both populations and a marked delay in the increase in microbial PAH degraders (Fig. 1). This difference in behavior is consistent with the kinetics of TPH depletion observed during the early stage (Table 2). As shown in Table 2, a higher TPH degradation rate was observed for treatments to which nutrients were added. In contrast, the proportion of the PAH-degrading microbial population compared to the heterotrophic population for the treatment without nutrients increased noticeably at 21 and 45 days and reached 100% at 135 days, while lower proportions were observed for treatments with nutrients (Fig. 1). In addition, at the end of the experiment a larger PAH-degrading microbial population was observed for the treatment without nutrients. Thus, the majority presence of microbial PAH degraders during the late stage could be linked to the higher TPH degradation rates observed, especially with more recalcitrant PAHs. Both changes in PAH bioavailability and enrichment of more recalcitrant PAHs could change the microbial population and the multisubstrate interactions (8, 9, 14, 22).

We found 13 different genera that were related to DGGE excised bands during biostimulation of a heavily PAH-contaminated soil: *Sphingomonas*, *Azospirillum*, *Roseomonas*, *Brevundimonas*, *Trojanella*, *Agrobacterium*, *Alcaligenes*, *Xanthomonas*, *Achromobacter*, *Sinorhizobium*, *Erytrobacter*, *Cytophaga*, and *Rhodococcus*.

During the first stage of biodegradation in the 2M treatment and the 4M treatment, the *Sphingomonas* and *Azospirillum* phylotypes (α-*Proteoabacteria*) were the dominant taxa (Table 4). Furthermore, the only two coincident DGGE bands for the two treatments belong to these phylotypes (B2-11 = B4-12 and B2-20 = B4-24). Therefore, taking into account that with both treatments high levels of TPH and PAH biodegradation were observed during the first 90 days, these phylotypes may be linked to the fast biodegradation observed for acenaphthene, fluorene, phenanthrene, anthracene, alkyl-phenanthrenes, fluoranthene, and pyrene. These results are consistent with those of Roling-Wilfred et al. (29) and Kasai et al. (19), who observed strong dominance of α-*Proteobacteria* in bacterial communities found in recently spilled oil in Nakhodka and in oil-spiked intertidal sediments after 6 days, respectively.

During data analysis, a high abundance of gram-negative bacteria was observed that could have been due to the extraction bias. However, the extraction method used in this study was able to extract DNA from gram-positive bacteria, such as *Rhodococcus* (this study), *Mycobacterium*, and *Bacillus* laboratory strains, suggesting that gram-negative bacteria dominated the creosote-contaminated soil during the bioremediation process.

Bioaugmentation assay. For the bioaugmentation treatment (treatment 6M), no differences in the rates of biodegradation of TPH and PAHs or in community structure determined by PCR-DGGE and MPN analysis were detected. In a previous study (36) we observed that the PAH-degrading capability of consortium AM (used as the inoculum in the present study) was not affected after growth in rich media. Also, this consortium contained 19 microbial components identified as *Sphingomonas*, *Pseudomonas*, *Stenotrophomonas*, *Ochrobactrum*, *Alcaligenes*, *Pandorea*, *Labrys*, and *Fusarium* (37). As shown in Fig. 5, none of the visible bands from consortium AM comigrated with bands from inoculated soil (treatment 6M), indicating that the inoculated microorganisms did not compete favorably with the indigenous bacterial community, even though they were originally from a PAH-contaminated soil (36) and the inoculum size was at least equal to (10^8 MPN g of $soil^{-1}$), if not larger than, the indigenous population and organisms were periodically inoculated throughout the experiment (Table 1). Moreover, the microbial population structure of inoculated soil was very similar to that of the soil biostimulated with nutrients during the first 45 days, in which the maximum biodegradation rates were observed. Therefore, the indigenous population changed independent of the inoculum, indicating that the biodegradation process was probably the strongest selection factor for the shifts in the microbial population.

Conclusions. This study showed that specific phylotypes of bacteria are related both to inorganic nutrient addition to the soil and to different phases of PAH degradation in a nonspiked PAH-contaminated soil, and it highlighted the importance of understanding how interspecies interactions, nutrient effects, and changes in PAH bioavailability and recalcitrance influence the degradation capability and structure of a microbial community.

ACKNOWLEDGMENTS

This research was funded by grants from the Spanish Government's National Plan for Research (REN2001-3425/TECNO; PPQ-2000-0105-P4 and 2001SGR 00143) and CIRIT 2001SGR 00143. M.V. received a postgraduate fellowship from the Comissionat de Recerca i Innovació Tecnològica (CIRIT) of the Generalitat de Catalunya.

We declare that the experiments discussed in this paper complied with current Spanish law.

REFERENCES

1. **Abalos, A., M. Viñas, J. Sabaté, M. A. Manresa, and A. M. Solanas.** 2004. Enhanced biodegradation of Casablanca crude oil by a microbial consortium in presence of a rhamnolipid produced by *Pseudomonas aeruginosa* AT10. Biodegradation **15:**249–260.
2. **Alexander, M.** 1999. Biodegradation and bioremediation, 2nd ed. Academic Press, Inc., San Diego, Calif.
3. **Alexander, M.** 2000. Aging, bioavailability, and overestimation of risk from environmental pollutants. Environ. Sci. Technol. **34:**4259–4265.
4. **Altschul, S. F., W. Gish, W., Miller, E. W. Meyers, and D. J. Lipman.** 1990. Basic local alignment search tool. J. Microbiol. Methods **215:**403–410.

5. **Amann, R. I., W. Ludwig, and K. H. Schleifer.** 1995. Phylogenetic identification and in situ detection of individual microbial cells without cultivation. Microbiol. Rev. **59:**143–169.
6. **Andreoni, V., L. Cavalca, M. A. Rao, G. Nocerino, S. Bernasconi, E. Dell'Amico, M. Colombo, and L. Gianfreda.** 2004. Bacterial communities and enzyme activities of PAHs polluted soils. Chemosphere **57:**401–412.
7. **Atagana, H. I.** 2004. Bioremediation of creosote-contaminated soil in South Africa by landfarming. J. Appl. Microbiol. **96:**510–520.
8. **Bastiaens, L., D. Springael, P. Wattiau, H. Harms, R. Dewachter, H. Verachtert, and L. Diels.** 2000. Isolation of adherent polycyclic aromatic hydrocarbon (PAH)-degrading bacteria using PAH-sorbing carriers. Appl. Environ. Microbiol. **66:**1834–1843.
9. **Bodour, A. A., J. M. Wang, M. L. Brusseau, and R. M. Maier.** 2003. Temporal change in culturable phenanthrene degraders in response to long-term exposure to phenanthrene in a soil column system. Environ. Microbiol. **5:**888–895.
10. **Braddock, J. F., M. L. Ruth, P. H. Catterall, J. L. Walworth, and K. A. McCarthynd.** 1997. Enhancement and inhibition of microbial activity in hydrocarbon-contaminated arctic soils: implications for nutrient-amended bioremediation. Environ. Sci. Technol. **31:**2078–2084.
11. **Casellas, M., M. Grifoll, J. M. Bayona, and A. M. Solanas.** 1997. New metabolites in the degradation of fluorene by *Arthrobacter* sp. strain F101. Appl. Environ. Microbiol. **63:**819–826.
12. **Eriksson, M., G. Dalhammar, and A. K. Borg-Karlson.** 2000. Biological degradation of selected hydrocarbons in an old PAH/creosote contaminated soil from a gas work site. Appl. Microbiol. Biotechnol. **53:**619–626.
13. **Fernandez, P., M. Grifoll, A. M. Solanas, J. M. Bayona, and J. Albaigés.** 1992. Bioassay-directed chemical analysis of genotoxic components in coastal sediments. Environ. Sci. Technol. **26:**817–829.
14. **Friedrich, M., R. J. Grosser, E. A. Kern, W. P. Inskeep, and D. M. Ward.** 2000. Effect of model sorptive phases on phenanthrene biodegradation: molecular analysis of enrichments and isolates suggests selection based on bioavailability. Appl. Environ. Microbiol. **66:**2703–2710.
15. **Fromin, N., J. Hamelin, S. Tarnawski, D. Roesti, K. Jourdain-Miserez, N. Forestier, S. Teyssier-Cuvelle, F. Gillet, M. Aragno, and P. Rossi.** 2002. Statistical analysis of denaturing gel electrophoresis (DGE) fingerprinting patterns. Environ. Microbiol. **4:**634–643.
16. **Gee, G. W., and J. W. Bauder.** 1986. Particle-size analysis. Methods of soil analysis. Part 1. Physical and mineralogical methods, p. 383–411. American Society of Agronomy, Inc., and Soil Science Society of America, Inc., Madison, Wis.
17. **Hall, T. A.** 1999. BioEdit: a user-friendly biological sequence alignment editor and analysis program for Windows 95/98/NT. Nucleic Acids Symp. **41:**95–98.
18. **Kaplan, C. W., and C. L. Kitts.** 2004. Bacterial succession in a petroleum land treatment unit. Appl. Environ. Microbiol. **70:**1777–1786.
19. **Kasai, Y., H. Kishira, K. Syutsubo, and S. Harayama.** 2001. Molecular detection of marine bacterial populations on beaches contaminated by the Nakhodka tanker oil-spill accident. Environ. Microbiol. **3:**246–255.
20. **Kazunga, C., and M. D. Aitken.** 2000. Products from the incomplete metabolism of pyrene by polycyclic aromatic hydrocarbon-degrading bacteria. Appl. Environ. Microbiol. **66:**1917–1922.
21. **Kazunga, C., M. D. Aitken, A. Gold, and R. Sangaiah.** 2001. Fluoranthene-2,3- and -1,5-diones are novel products from the bacterial transformation of fluoranthene. Environ. Sci. Technol. **35:**917–922.
22. **Lotfabad, S. K., and M. R. Gray.** 2002. Kinetics of biodegradation of mixtures of polycyclic aromatic hydrocarbons. Appl. Microbiol. Biotechnol. **60:** 361–366.
23. **Macnaughton, S. J., J. R. Stephen, A. D. Venosa, G. A. Davis, Y. J. Chang, and D. C. White.** 1999. Microbial population changes during bioremediation of an experimental oil spill. Appl. Environ. Microbiol. **65:**3566–3574.
24. **Maidak, B. L., J. R. Cole, T. G. Lilburn, C. T. Parker, Jr., P. R. Saxman, J. M. Stredwick, G. M. Garrity, B. Li, G. J. Olsen, S. Pramanik, T. M. Schmidt, and J. M. Tiedje.** 2000. The RDP (Ribosomal Database Project) continues. Nucleic Acid Res. **28:**173–174.
25. **Muyzer, G., E. D. De Waal, and A. G. Uitterlinden.** 1993. Profiling of complex microbial populations by denaturing gradient gel electrophoresis analysis of polymerase chain reaction-amplified genes coding for 16S rRNA. Appl. Environ. Microbiol. **59:**695–700.
26. **Nogales, B., E. R. B. Moore, E. Llobet-Brossa, R. Rossello-Mora, R. Amann, and K. N. Timmis.** 2001. Combined use of 16S ribosomal DNA and 16S rRNA to study the bacterial community of polychlorinated biphenyl-polluted soil. Appl. Environ. Microbiol. **67:**1874–1884.
27. **Rhykerd, R. L., R. W. Weaver, and K. J. McInnes.** 1995. Influence of salinity on bioremediation of oil in soil. Environ. Pollut. **90:**127–130.
28. **Ringelberg, D. B., J. W. Talley, E. J. Perkins, S. G. Tucker, R. G. Luthy, E. J. Bouwer, and H. L. Fredrickson.** 2001. Succession of phenotypic, genotypic, and metabolic community characteristics during in vitro bioslurry treatment of polycyclic aromatic hydrocarbon-contaminated sediments. Appl. Environ. Microbiol. **67:**1542–1550.
29. **Roling-Wilfred, F. M., M. G. Milner, D. M. Jones, K. Lee, F. Daniel, J. P. Swannell-Richard, and I. M. Head.** 2002. Robust hydrocarbon degradation and dynamics of bacterial communities during nutrient-enhanced oil spill bioremediation. Appl. Environ. Microbiol. **68:**5537–5548.
30. **Sabaté, J., M. Viñas, and A. M. Solanas.** 2004. Laboratory-scale bioremediation experiments on hydrocarbon-contaminated soils. Int. Biodeterior. Biodegrad. **54:**19–25.
31. **Sabaté, J., M. Viñas, and A. M. Solanas.** Bioavailability assessment and environmental fate of PAHs in biostimulated creosote-contaminated soil. Chemosphere, in press.
32. **Siciliano, S. D., J. J. Germida, K. Banks, and C. W. Greer.** 2003. Changes in microbial community composition and function during a polyaromatic hydrocarbon phytoremediation field trial. Appl. Environ. Microbiol. **69:** 483–489.
33. **Solanas, A. M.** 1988. Contaminación y biodegradación de hidrocarburos en las aguas superficiales del Barcelonés. Thesis. Department of Microbiology, University of Barcelona, Barcelona, Spain.
34. **Torsvik, V., L. Ovreas, and T. F. Thingstad.** 2002. Prokaryotic diversity-magnitude dynamics, and controlling factors. Science **296:**1064–1066.
35. **Venosa, A. D., M. T. Suidan, B. A. Wrenn, K. L. Strohmeier, J. R. Haines, B. L. Eberhart, D. King, and E. Holder.** 1996. Bioremediation of an experimental oil spill on the shoreline of Delaware Bay. Environ. Sci. Technol. **30:**1764–1775.
36. **Viñas, M., M. Grifoll, J. Sabate, and A. M. Solanas.** 2002. Biodegradation of a crude oil by three microbial consortia of different origins and metabolic capabilities. J. Ind. Microbiol. Biotechnol. **28:**252–260.
37. **Viñas, M., J. Sabaté, C. Guasp, J. Lalucat, and A. M. Solanas.** Culture-dependent and -independent approaches establish the complexity of a PAH-degrading microbial consortium. Can. J. Microbiol., in press.
38. **Walworth, J. L., and C. M. Reynolds.** 1995. Bioremediation of a petroleum-contaminated cryic soil: effects of phosphorus, nitrogen, and temperature. J. Soil Contam. **4:**299–310.
39. **Wrenn, B. A., and A. D. Venosa.** 1996. Selective enumeration of aromatic and aliphatic hydrocarbon-degrading bacteria by a most-probable-number procedure. Can. J. Microbiol. **42:**252–258.
40. **Yu, Z., and M. Morrison.** 2004. Comparisons of different hypervariable regions of *rrs* genes for use in fingerprinting of microbial communities by PCR-denaturing gradient gel electrophoresis. Appl. Environ. Microbiol. **70:** 4800–4806.
41. **Zucchi, M., L. Angiolini, S. Borin, L. Brusetti, N. Dietrich, C. Gigliotti, P. Barbieri, C. Sorlini, and D. Daffonchio.** 2003. Response of bacterial community during bioremediation of an oil-polluted soil. J. Appl. Microbiol. **94:**248–257.